MICROSTRUCTURE AND TENSILE PROPERTIES OF EXTRUDED 7475 AL-AL_2O_3 PARTICLE COMPOSITES

A. Daoud [1], W. Reif [2] and P. Rohatgi [3]

1 Composite materials lab., Central Metallurgical Research and Development Institute, Helwan, Cairo, Egypt
2 Institut für Metallische Werkstoffe-Metallkunde, TU Berlin, Berlin, Germany
3 Materials Department, University of Wisconsin-Milwaukee, 3200 N. Cramer Street, Milwaukee, WI 53201, USA

ABSTRACT

7475 Al alloy reinforced with Al_2O_3 particulates of different sizes (25 μm angular or 40 μm microsphere) and volume fractions were successfully produced using vortex method followed by extrusion. SEM and energy dispersive X-ray analysis (EDXA) taken from the extracted Al_2O_3 particulate revealed that the particulate reacted with the molten 7475 Al during melting and casting to form a layer of $MgAl_2O_3$ spinel at the interface. Microstructural parameters, such as volume fraction, size and shape of the particulates, were correlated with the ambient and elevated (200 ^{o} C) temperature tensile properties as well as failure mechanisms. At both temperatures, the composite had higher yield strength than the unreinforced alloy, increasing with increasing the particulate volume fraction. The elongation was lower in the composite, decreasing with increasing level of reinforcement and increasing with increasing temperature. The Al_2O_3 particulate size had a marginal effect (within the particulate size range studied here) on the tensile properties. Although these composites exhibited limited ductility on a macroscopic scale, fractography revealed that fractures occurred by a locally ductile mechanism. The microstructural damage in the composites also varied with the temperature: particulate fracture dominated at ambient temperature and interfacial debonding and particulate fracture were the main damage features at elevated temperature.

1. INTRODUCTION

Aluminum-based matrix composites reinforced with ceramic particles offer significant increases in stiffness and strength over their monolithic alloy counterparts, and in recent years have been the focus of intensive efforts aimed at understanding the relation between processing and properties of these materials. Metal matrix composites (MMCs) can be synthesized using a number of techniques. These techniques can be broadly classified as: a) liquid phase techniques (or ingot metallurgy), b) semi-solid phase techniques and c) solid phase techniques [1,2]. Most of the fabrication methods exiting today have one thing is common; they are all too expensive and complicated, which limits the use of the MMCs. Moreover, foundry companies require MMCs to be formed by the same conventional techniques usually applied to the manufacturing of commercial components. Liquid phase route is the most economically viable amongst all the routes for MMCs production. In addition, this process allows very large size components to be fabricated. Stir casting route is the most promising one for synthesizing discontinuous reinforcement aluminum matrix composites because of its relative simplicity and easy adaptability with all shape casting processes used in metal casting industry [3, 4]. A number of secondary processes can be applied to MMC, usually with the objectives of consolidation (porosity elimination), improving the particulates distribution and/or forming into a required shape. These involve high temperature and large strain deformations. Extrusion is an attractive processing route for a class of materials which has typically been amongst the most difficult to work successfully [5].

Accordingly, the present work was undertaken to synthesize aluminum matrix alloy (7475 Al) reinforced with Al_2O_3 particulates of different sizes and volume fractions by using stir casting technique followed by extrusion. Microstructural characterization studies were carried out to establish the feasibility of the processing parameters. The microstructural parameters, such as the volume fraction and size of the particulates, were correlated with the ambient and elevated temperature tensile properties. Finally, more light was shed on the failure mechanisms operative in such composites so as to aid in the correlation of microstructure and properties of such composites.

2. EXPERIMENTAL PROCEDURES

7475 Al alloy reinforced with Al_2O_3 particles of different sizes (25 or 40 μm) and volume fractions (10, 15 or 25 vol.%) were produced using stir casting technique. The cast billets of the 7475 Al-Al_2O_3 composites as well as the matrix alloy were homogenized at 460 ^oC for 24 hrs, machined and used for extrusion process. The specimen used for extrusion had a diameter of 29.4 mm and a height of 95 mm. To reduce the maximum value of extrusion force, the specimen was tapered with half the die angle ($\alpha/2 = 75^o$) on one side. Hot extrusion was carried out by uniaxial pressing (50 ton) at a nominal temperature of 440 ^oC. The billet was held at the extrusion temperature for 30 mins before extrusion. The container is made of carbon tool steel and the punch and the die are of high speed steel. The inside of the container is carbon coated for lubrication. The die half angle α was 75^o and the extrusion speed was 1 mm/s. The extrusion ratio was about 10; thus, extruded rod 9.5 mm in diameter was obtained. Metallographic samples were cut from the cast and extruded 7475 Al-Al_2O_3 composites, sections from both longitudinal and transverse directions were cut from the extruded materials, mounted and ground using grades of SiC papers (79, 50, 38 and 8 μm), followed by polishing with (6, 3 and 1/4 μm) diamond paste. After that, the samples were etched with Keller's reagents to reveal the morphology and various structure characteristics. The samples were examined under optical microscope and DSM 950 scanning electron microscope (SEM). Compositional spot analyses were performed in and around the particulates as well as element distribution maps through the particulates and their surroundings using an energy dispersive X-ray analysis (EDXA) facility in the SEM.

Tensile specimens were cut from the extruded 7475 Al-Al_2O_3 composites with the tensile axes parallel to the extrusion direction. The specimen had a gauge length of 25 mm and a diameter of 4 mm with threaded ends, in accordance with the DIN 50125-B 4x20 requirements. The materials were tested in the peak aged (T6-temper) condition according to the following procedures. The specimens were solutionized at 510 ^oC for 2 hrs, water quenched at room temperature and subsequently aged at 120 ^oC. Tensile tests were done using an Instron 4112 testing machine equipped with Date Acquisition System that supplied the stress-strain date during testing. The tests were carried out at an initial strain rate of $3x10^{-4}$ s^{-1} at room and elevated (200 ^oC) temperatures. The specimens were held at the test temperature for 10 mins before testing. Three valid tests were performed for each material and tensile properties including o.1% and 0.2% yield strength, ultimate tensile strength, and elongation to fracture were derived. Owing to the low ductility of the composites, 0.1% yield strength was generally considered. Where possible, the 0.2% yield strength was also measured. After tensile testing, fractured specimens were gold coated and examined by SEM. The microstructural damage associated with the deformation was examined on longitudinal polished surface through the fracture.

3. RESULTS AND DISCUSSION

3.1 Microstructures

Representative optical micrographs of the hot extruded 7475 Al-Al_2O_3 particulate composites in the extrusion direction are shown in Fig. 1(a-d). The porosity was minimized significantly compared with the as-cast material. An improvement in the distribution of Al_2O_3 particulates was also achieved. This improvement was particularly evident in the composites reinforced with microsphere Al_2O_3 particulates, Fig. 1(d). An improvement in the distribution of particulates is desirable since it assists in eliminating the stress concentration sites arising from the particulates clustering and thus leads to an improvement in mechanical behavior compared with the as-cast material.

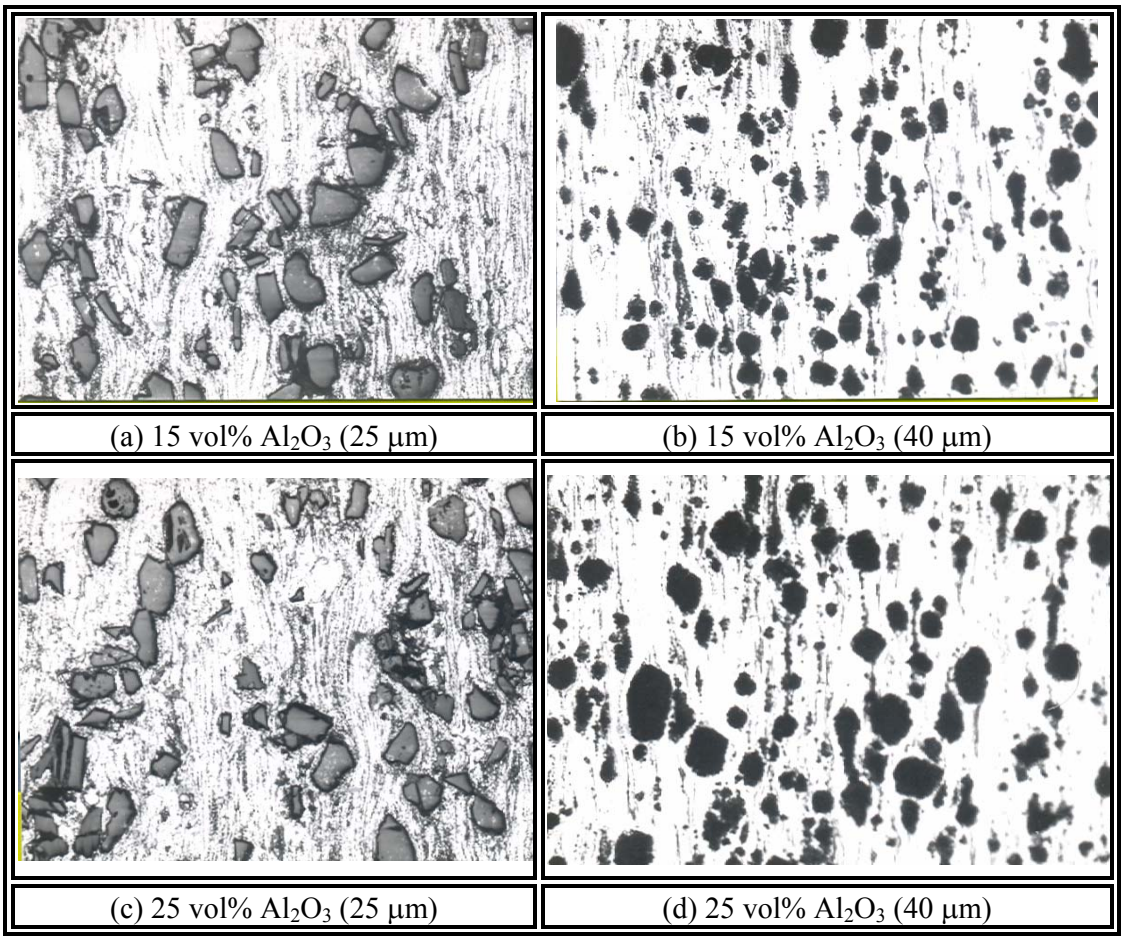

Figure 1: Extruded microstructures of 7475 Al alloy reinforced with different percentages of 25 μm angular or 40 μm (nominal) microsphere Al_2O_3 particulates

Other microstructural features of the extruded composites have attracted attention, notably the formation of Al_2O_3-enriched 'bands' parallel to the extrusion direction axis, Fig. 2(a). The migration of particulates must involve their displacement with respect to the surrounding matrix material. This means that the flow pattern of the extrusion by itself cannot explain the observed effects kinematically. The loading present during extrusion consists of a hydrostatic pressure added to a shear. The high shear

deformation produces some heat locally and thus temperature gradients, which generate flow stress gradients [6].

It is also observed that the presence of the Al_2O_3 particulates in the composite leads to heterogeneous matrix deformation during the extrusion. The matrix was observed to flow around the Al_2O_3 particulates. Localized matrix flow in the vicinity of the Al_2O_3 particulates was examined more closely using higher magnification, Fig. 2 (b). The matrix was severely deformed around the Al_2O_3 particulates, especially at both the sharp ends of angular particulates and in the vicinity of particulate clusters.

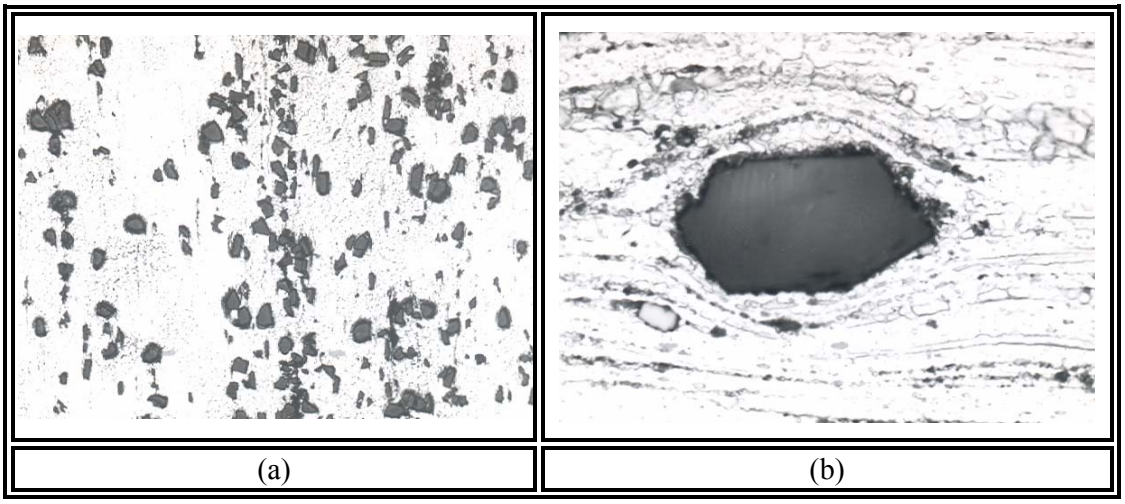

Figure 2: Micrographs showing formation of Al_2O_3-rich bands during extrusion (a) and severely distorted matrix around the Al_2O_3 particulate (b)

3.2 Interactions between Al_2O_3 particulates and 7475 Al alloy

Figure 3 is the SEM image of the extracted Al_2O_3 particulate, showing interfacial reaction products covering the surface of the particulate. Magnified view of Al_2O_3 particulate and the details of reaction products on its surface are presented in Fig. 3 (b). EDXA obtained from the reaction products shows the presence of excess Cu, Mg and O on the particulate surface compared to the matrix alloy, Fig. 4. Possible reactions are (free energy change values obtained from Ref. 7 and 8 for Al4.5Cu2Mg):

$3\,Mg(l) + Al_2O_3(s) = 3MgO\,(s) + 2Al(l)$ (1) $\Delta G = -39$ KJ/mole at 900 K

$MgO(s) + Al_2O_3(s) = MgAl_2O_4(s)$ (2) $\Delta G = -28$ KJ/mole at 900 K

$Mg(l) + 4/3\,Al_2O_3(s) = MgAl_2O_4(s) + 2/3\,Al(l)$ (3) $\Delta G = -41$ KJ/mole at 900 K

$Cu\,(l) + 1/2O_2(g) + Al_2O_3\,(s) = CuAl_2O_4(s)$ (4) $\Delta G = -33$ KJ/mole at 900 K

l: liquid and S: solid

The formation of $MgAl_2O_4$ spinel is energetically more favorable (reaction 3) in comparison with formation of MgO (reaction 1). Although spinel can form by reaction of Al_2O_3 and MgO, which is produced from direct oxidation of Mg in the melt, this process is kinetically very slow because it involves solid state reaction. Thus, the reaction given by equation 2 is considered unlikely. Reaction 3 describes the formation of the $MgAl_2O_4$ spinel as a result of direct reaction between the Al_2O_3 and Mg within the liquid matrix alloy. Hence, it is a likely mechanism for the formation of the spinel reaction product. The presence of Cu at particulates/matrix interface (Fig. 4 (a)) could be explained by the formation of cupric aluminate ($CuAl_2O_4$) at the particulate surface according to reaction 4. But, the formation of $CuAl_2O_4$ at particulates/matrix interface

may be hindered by the presence of Mg that preferentially reacts with O_2 to form $MgAl_2O_4$ spinel.

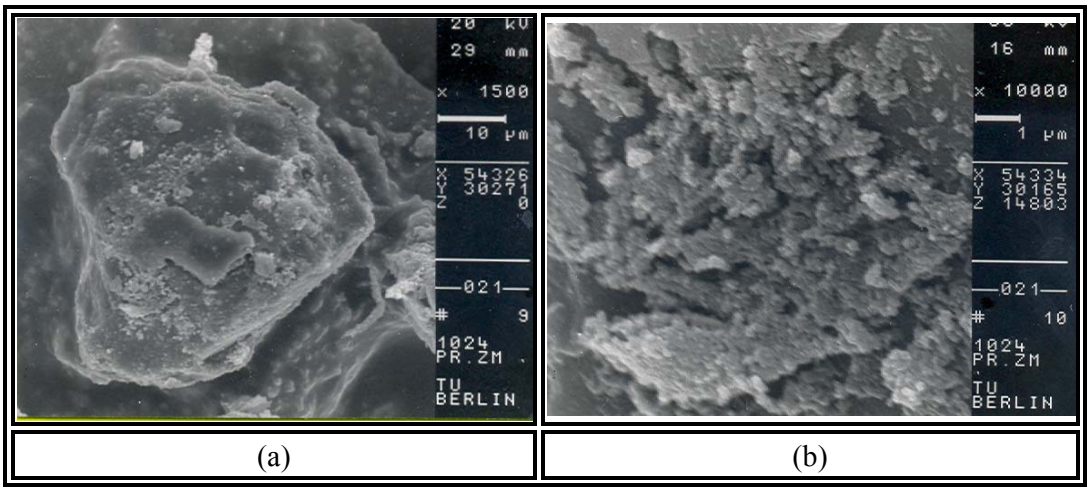

Figure 3: SEM micrographs of the Al_2O_3 particulate covered with reaction products (a) and magnified view of the reaction products (b)

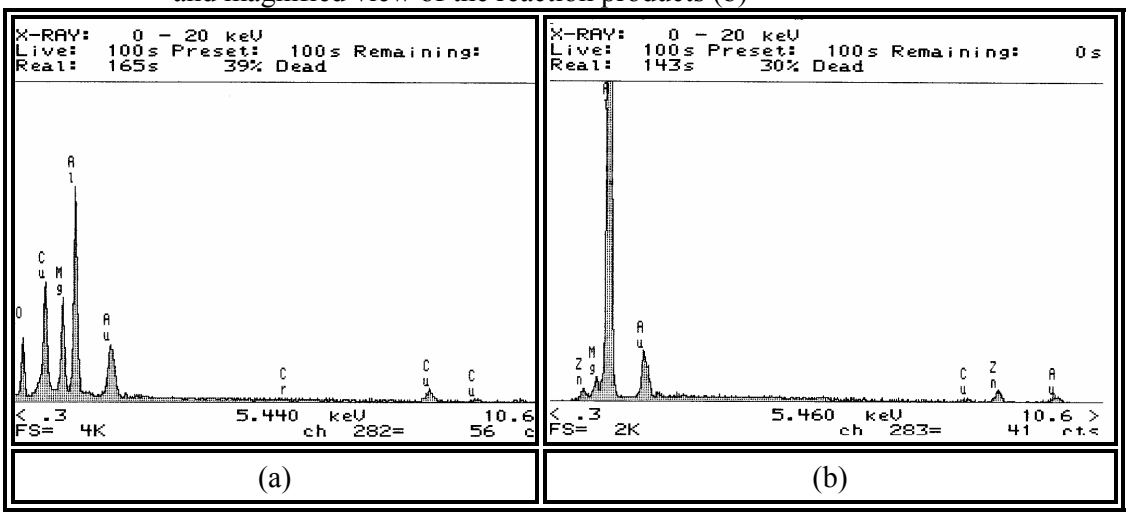

Figure 4: EDXA spectra taken from the reaction products (a) and 7475 Al matrix alloy (b)

3.3 Tensile properties

The ambient-temperature tensile properties of 7475 Al-Al_2O_3 particulate composites are shown in Table 1. The results reveal that the addition of Al_2O_3 particulates to the base alloy increases the 0.1% and 0.2% yield strength, but considerably reduces the ultimate tensile strength and strain to failure. As expected, the volume fraction of the particulates has a significant effect on the yield and ultimate strength. As the volume fraction of the particulates increases, the 0.1% and 0.2% yield strength increase. However, the ultimate strength and strain to failure decrease as the volume fraction of the particulates increases. The Al_2O_3 particulate size has a little effect on the tensile properties. It should be mentioned that in case of 40 µm microsphere particulates reinforced 7475 Al alloy, the mean particulate size is reduced by extrusion (Fig. 1 and 2). Thus, the average particulate sizes become nearly the same in both cases (angular and microsphere particulates) after extrusion. Consequently, it is expected that the size of Al_2O_3

particulate has little effect on the tensile properties in the present investigation. It is worth noting that the ultimate tensile strength of the composite samples is slightly higher than the yield strength, indicating that the work hardening rate after yielding is small. The possible explanation for this is that the size of the particulates in the present composites is too large (25 or 40 μm compared to < 5 μm in other studies) and these large particulates are not only unable to pin dislocations but also have low strengthening ability [9]. Moreover, the composite failed in a brittle manner, with ultimate strength related to its failure strain. The ultimate strength decreases with increasing Al_2O_3 particulates content because the composite is not able to exhibit enough ductility to attain full ultimate tensile strength. This means that the matrix probably does not have a sufficient internal ductility to redistribute the very high localized internal stresses. Hence, the composite failed before being able to reach stable flow and normal ultimate strength. Moreover, the presence of the Al_2O_3 particulates restricts the plastic flow of the matrix, initiating failure at lower strains by the formation of cavities in the vicinity of the particulates.

Table 1: Tensile properties at room temperature (R.T) and 200 ^oC (E.T.) of the composites

Matrix	Al_2O_3 size (μm)	Al_2O_3 vol%	0.1% yield strength (MPa)		0.2 % yield strength (MPa)		Ultimate strength (MPa)		Elongation (%)	
			R.T	E.T.	R.T	E.T.	R.T	E.T.	R.T	E.T.
7475 Al	-	0	400	278	457	349	580	474	10	33
7475 Al	25	10	410	356	471	370	501	414	2.8	13
7475 Al	25	15	421	360	485	379	490	390	2.25	10.8
7475 Al	25	25	443	370	490	380	495	387	2.01	10.6
7475 Al	40	10	410	344	460	367	480	402	2.9	14.3
7475 Al	40	15	427	365	477	374	499	398	2.8	13.5
7475 Al	40	25	435	370	480	374	487	380	2.6	11.3

Table 1 presents the tensile properties of the 7475 Al- Al_2O_3 particulate composites tested at 200 ^oC. The ultimate tensile strength of both the matrix and the composites dropdowns remarkably at high temperature. However, the yield strength of the composite shows a better performance than that of the matrix. The yield strength increases with increasing the volume of the reinforcement. The elongation is lower in the composite than that in the matrix, increasing with increasing temperature and decreasing with increasing volume of reinforcement. In addition, the composite presents an improvement in the ultimate tensile strength compared to that of the composite at room temperature because the Al_2O_3 particulates come to act as reinforcements due to the higher deformation suffered by the matrix in comparison with its behavior at room temperature. Generally, the strengthening effects, which can occur in the composite materials, can be divided into two groups. Those by which the reinforcement directly contributes to the material strength and those where by an indirect strengthening of the matrix is achieved [9-13].

3.4 Fractogrphy

The fracture surface of the 7475 Al matrix tested at room temperature shown in Fig. 5(a) reveals predominantly transgranular rupture with dimples and heavy shear deformation. The specimen shows evidence of having a greater amount of plastic

deformation during cracking, consistent with the high ductility.The general features associated with fracture of these composites can be summarized in terms of macroscopically brittle behavior of the specimens, which fractured without any evidence of necking. However, SEM fractographs revealed that the fracture occurred by a locally ductile mechanism, resulting in the formation of dimples. The fractographs of the 7475 Al composites with 25 μm Al_2O_3 particulates are shown in Fig. 5 (b, c). The fracture surface essentially consists of a bimodel distribution of flat dimples associated with the Al_2O_3 particulates and small dimples associated with ductile failure of the 7475 Al matrix. In most cases, the large dimples contain Al_2O_3 particulates and are of the size as the particulates responsible for their formation. In addition, a large number of Al_2O_3 particulates, some of them covered by metallic matrix, is seen in the micrographs (Fig. 5(b, c)). The observation of particulate surface shows smooth planer particulate surfaces which indicates that this portion of the particulate was cut rather than decohered. This suggests that the interface is strong, which is also evidenced by the torn-off matrix left on the interface.

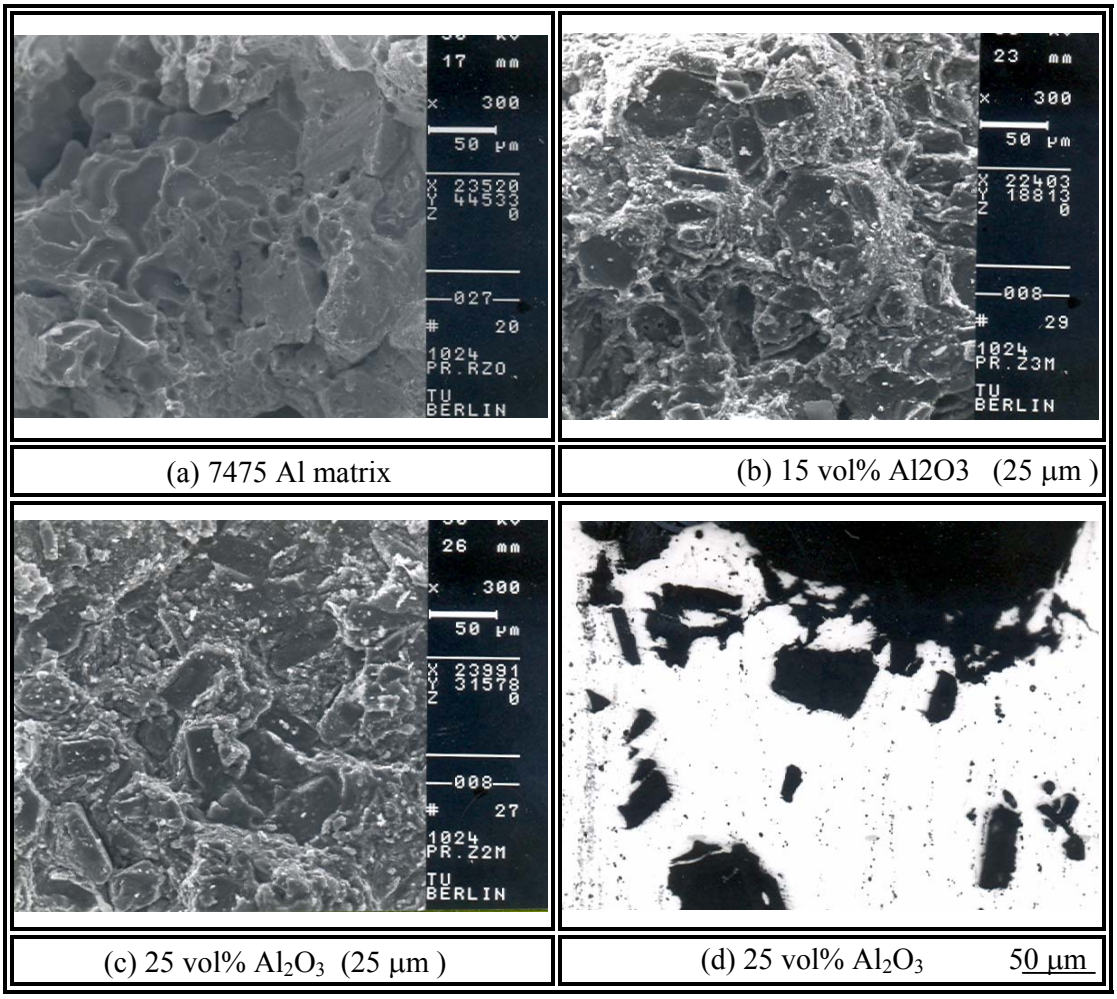

(a) 7475 Al matrix

(b) 15 vol% Al2O3 (25 μm)

(c) 25 vol% Al_2O_3 (25 μm)

(d) 25 vol% Al_2O_3 50 μm

Figure 5: SEM micrographs of fracture surfaces (a, b, c) and optical micrographs of longitudinal sections beneath the fracture surfaces of 7475 Al alloy reinforced with 25 μm Al_2O_3 tested at room temperature (d)

Figure 5(d) is the microstructure beneath the fracture surfaces of the composite tensile sample. It can be observed in the area close to the fracture surface that there are some broken Al_2O_3 particulates. The direction of the internal cracks within the Al_2O_3 particulates is normal to the loading axis regardless of the particulate orientation. From these observations, it is deduced that cracks were initiated by microvoids formed at sites of broken Al_2O_3 particulates or at the near vicinity of the Al_2O_3 /matrix interface, followed by deformation of the surrounding matrix (i.e., void growth) forming ligaments between neighboring voids. Subsequently, void coalescence occurred by breaking of ligaments resulting in crack propagation in the matrix or near vicinity of the Al_2O_3 /matrix interface, leaving behind, on the fracture surface, the familiar hemispheroidal cavities, i.e. dimples.

The initiation or propagation of a crack in the near vicinity of the Al_2O_3/matrix interface, as observed in the fractograph of the broken particulates that are coated with the matrix material (Fig. 5(c, b)), can be attributed to the lowering of the matrix strength as a result of reduction in alloying elements concentration in the near vicinity of the interface as well as matrix inability to accommodate a large plastic deformation with concomitant stress concentration in this region. The broken ligaments between neighboring dimples in 7475 Al- 10 vol% Al_2O_3 material appear to be longer than those in 7475 Al-25 vol% Al_2O_3, consistent with the better ductility of the material with less Al_2O_3 particulates.

SEM observations of the fractured specimens of the 7475 Al-Al_2O_3 particulate composites tested at 200 ^oC as well as the 7475 Al matrix alloy are shown in Fig. 6(a-c). It can be seen that the unreinforced matrix shows predominantly transgranular rupture and evidence of having undergone a greater amount of plastic deformation during cracking, consistent with the enhanced ductility at high temperature. A bimodal distribution of voids intermingles with shallow dimples is evident on the transgranular fracture surface. The shallow dimples are the result of the presence of small second-phase intermetallic particulates, with the size of the dimples increasing with increasing the temperature. The fracture surfaces of the composites are found to consist of fine dimples, resulting from ductile failure of the matrix, large dimples, resulting from interfacial debonding of the particulates and some creaked particulates. The SEM fractographs also show extensive ductile dimpling in the matrix between the particulates. In addition, there are secondary cracks along the interface between the particulate and the matrix, Fig. 6(d). Some cracked particulates and dimples of the matrix alloy on the surface of the particulates can be observed, which confirms relatively good bonding of the interface at 200 ^oC, but a part of the original surface of the particulate can also be observed, Fig. 6(d). From Fig. 6(d) it can be seen that two regions of the microstructure are particularly susceptible to void nucleation: individual particulate ends and the region between closely spaced particulates. Individual particulate ends are regions of high matrix strain because the adjacent matrix is essentially free of constraint from adjacent particulates. It is worth noting that the scale of voiding in the unreinforced alloy is much coarser than any of the matrix fracture features observed in the composites. The above results reveal debonding Al_2O_3/matrix interface and cracking of Al_2O_3 particulate as two predominant failure modes at elevated temperature (200 ^oC). The results do not reveal any single dominant mechanism. Generally, all the composites show the same trends, with particulate fracture dominating the damage at room temperature, and interfacial debonding and particulate fracture becoming the main features at 200 ^oC. Particulate fracture depends on the local stress field on the particulate exceeding the particulate strength and since the particulate is the brittle, the particulate fracture strength is controlled by intrinsic

flaws. Consequently, larger particulates are more prone to crack since they have a higher probability to containing a critical flaw. However, at higher temperature, the local stresses are not large enough to fracture the particulates since the matrix flow stress decreases with increasing temperature and in this case all the strain has to be accommodated by the matrix. This results in normal stresses at the interface exceeding the interface strength and void nucleation14 [137]. In addition, the tensile elongations are much lower in the composites at room and elevated temperatures, which is consistent with the higher level of damage observed in the composites. A higher level of reinforcement results in a lower tensile elongation in the composites, particularly at room temperature where particulate cracking is the more dominant damage process prior to final fracture.

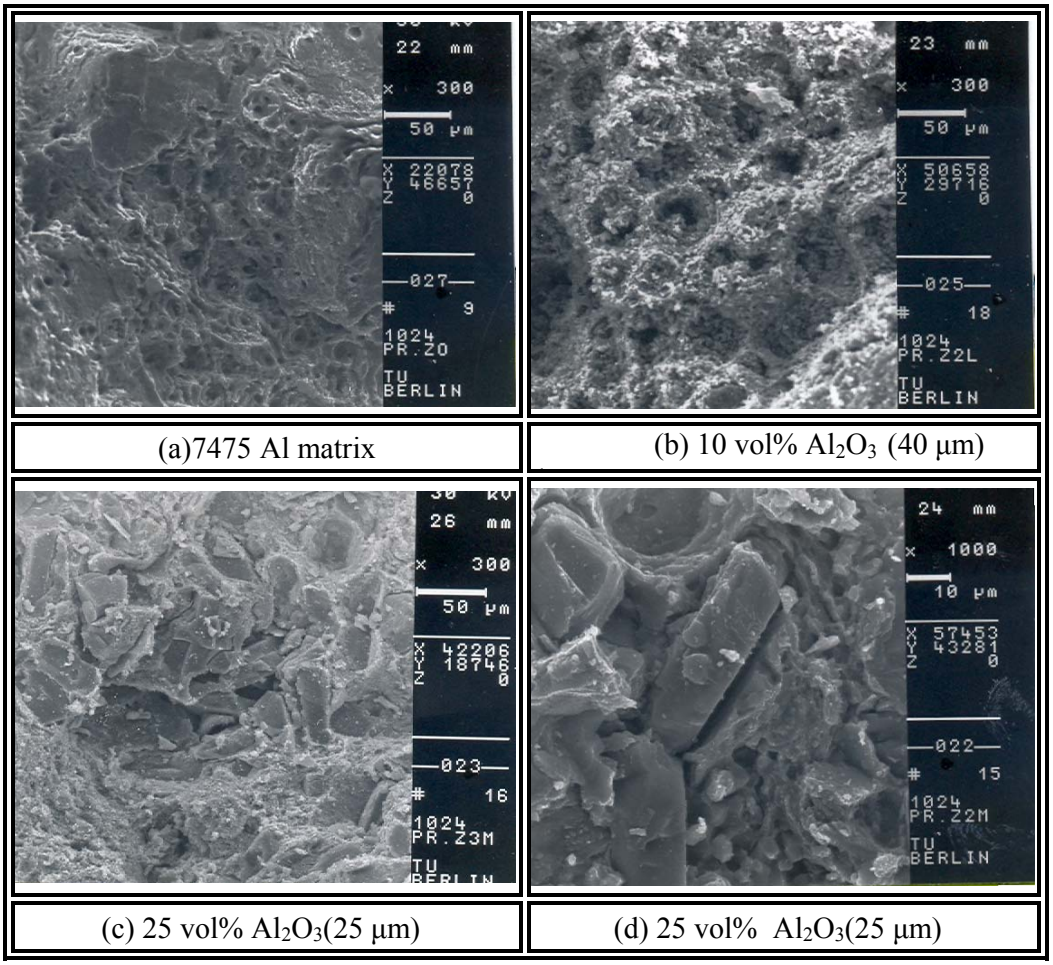

(a)7475 Al matrix | (b) 10 vol% Al_2O_3 (40 µm)

(c) 25 vol% Al_2O_3(25 µm) | (d) 25 vol% Al_2O_3(25 µm)

Figure 6: SEM micrographs of fracture surfaces of 7475 Al and 7475 Al reinforced with Al_2O_3 tested at 200 ^oC

4. CONCLUSIONS

7475 Al alloy based metal matrix composites containing Al_2O_3 particulates of different sizes (25 or 40 µm) and volume fractions (10, 15 or 25 vol. %) can be successfully produced using casting route followed by extrusion.

The Al_2O_3 particulates react with the molten A356 Al or 7475 Al during melting and casting to form a layer of $MgAl_2O_3$ spinel at the interface.

At ambient and elevated (200 ^{o}C) temperatures, the composite has higher yield strength than that of the unreinforced alloy. The elongation is lower in the composite, decreasing with increasing level of reinforcement and increasing with increasing temperature. The Al_2O_3 particulate size has a marginal effect (within the size range studied here) on the tensile properties

Although these composites exhibit limited ductility on a macroscopic scale, fractography revealed that fractured occurs by a locally ductile mechanism. Microstructural damage in the composites varies with the temperature: particulate fracture dominates at ambient temperature and interfacial debonding is the main damage feature at elevated temperature (200 ^{o}C).

REFERENCES

1- Mondal D.P., Ganesh N.V., Muneshwar V.S., Das S. and Ramakrishnan N., "Effect of SiC concentration and strain rate on the compressive deformation behaviour of 2014Al-SiCp composite", *Materials Science and Engineering: A*, 2006;433:18-31.

2- Ward P.J., Atkinson H.V., Anderson P.R.G., Elias L.G., Garcia B., Kahlen L. and Rodriguez-ibabe J-M., " Semi-solid processing of novel MMCs based on hypereutectic aluminium-silicon alloys", *Acta Materialia*,1996; 44: 1717-1727.

3- Ceschini L., Minak G. and Morri A. "Tensile and fatigue properties of the AA6061/20 vol.% Al_2O_{3p} and AA7005/10 vol.% Al_2O_3p composites", *Composites Science and Technology*, 2006; 66: 333-342.

4-Gupta M., Lai M.O. and Lim C.Y.H. "Development of a novel hybrid aluminum-based composite with enhanced properties", *Journal of Materials Processing Technology*, 2006;176: 191-199.

5- Tham L., Gupta M., M. and L., "Effect of reinforcement volume fraction on the evolution of reinforcement size during the extrusion of Al-SiC composites", Materials Science and Engineering A, 2002;326: 355-363.

6- Ehrstrom J.C. and Kool W.H., "Migration of particles during extrusion of metal matrix composites", *Journal of Materials Science Letters*, 1988; 7: 578- 580.

7- Y. Brechet, J. Newell, S.Tao and J.D. Embury, "A note on particle comminution at large plastic strains in Al-SiC composites", *Scripta Metallurgica et Materialia*,1993;28: 47-51.

8- Cappleman G.G., Watts J.F. and Clyne T.W., "The interface region in squeeze-infiltrated composites containing δ-alumina fibre in an aluminium matrix", *Journal of Materials Science* 1985;20: 2159-2168.

9- Arsenault R.J., Wang L. and Feng C.R., "Strengthening of composites due to microstructural changes in the matrix ", *Acta Metallurgica et Materialia*, 1991; 3, 47-57.

10- Aikin R.M. and Christodoulou L., "The role of equiaxed particles on the yield stress of composites ", *Scripta Metallurgica et Materialia*, 1991; 25, 9-14.

11- Taya M., Lulay K.E. and . Lloyd D.J, " Strengthening of a particulate metal matrix composite by quenching", *Acta Metallurgica et Materialia*, 1991; 39: 73-87

12- Miller W.S. and Humphreys F.J., " Strengthening mechanisms in particulate metal matrix composites", *Scripta Metallurgica et Materialia*,1991;25: 33-38

13- papazian J.M. and Adler P.N., " Tensile properties of short fiber-reinforced SiC/Ai composites: Part I. effects of matrix precipitates", *Metallurgical and Materials. Transactions. A*,1990; 21A:401-410.

14- Argon A.S., Im J. and Safoglu R., "Cavity formation from inclusions in ductile fracture" *Metallurgical and Materials Transactions. A*, 1975; 6A: 825-837.